DOI:10.1021/jf100135h

JOURNAL OF AGRICULTURAL AND FOOD CHEMISTRY
ARTICLE

Curcumin Nanoparticles Improve the Physicochemical Properties of Curcumin and Effectively Enhance Its Antioxidant and Antihepatoma Activities

Feng-Lin Yen,[†] Tzu-Hui Wu,[‡] Cheng-Wei Tzeng,[§] Liang-Tzung Lin,[#] and Chun-Ching Lin*[,§,⊥]

[†]Department of Fragrance and Cosmetics, College of Pharmacy, Kaohsiung Medical University, Kaohsiung, Taiwan, [‡]Health Bureau of Kaohsiung County Government, Kaohsiung, Taiwan, [§]Graduate Institute of Natural Products, College of Pharmacy, Kaohsiung Medical University, Kaohsiung, Taiwan, [#]Department of Microbiology and Immunology, Dalhousie University, Halifax, Nova Scotia, Canada, and [⊥]School of Pharmacy, College of Pharmacy, Kaohsiung Medical University, Kaohsiung, Taiwan

Curcumin (CUR), a natural polyphenol isolated from tumeric (*Curcuma longa*), has been documented to possess antioxidant and anticancer activities. Unfortunately, the compound has poor aqueous solubility, which results in poor bioavailability following high doses by oral administration. To improve the solubility of CUR, we developed a novel curcumin nanoparticle system (CURN) and investigated its physicochemical properties as well as its enhanced dissolution mechanism. Our results indicated that CURN improved the physicochemical properties of CUR, including a reduction in particle size and the formation of an amorphous state with hydrogen bonding, both of which increased the drug release of the compound. Moreover, in vitro studies indicated that CURN significantly enhanced the antioxidant and antihepatoma activities of CUR ($P < 0.05$). Consequently, we suggest that CURN can be used to reduce the dosage of CUR and improve its bioavailability and merits further investigation for therapeutic applications.

KEYWORDS: Curcumin; nanoparticle; physicochemical properties; antioxidant; antihepatoma

INTRODUCTION

It has been well documented that many active compounds in natural foods, including fruits and vegetables, possess bioactivities that can help prevent and cure diseases. Turmeric (*Curcuma longa*), a plant native to tropical South Asia, is commonly used as a food spice in curry and also as a medicine for the treatment of various diseases. Curcumin (CUR; **Figure 1**) is the major active polyphenol compound isolated from the dry rhizomes of *C. longa* (*1*), and this agent has been extensively investigated for its pharmacological activities that include anticancer, anti-inflammatory, antioxidant, antiulcer, immunomodulatory, wound healing, neuroprotective, and antiaging effects (*2*).

Despite the array of bioactivities that it possesses, curcumin has low bioavailability due to its poor aqueous solubility and dissolution properties (*3*). Several clinical trials have demonstrated that although a high dose of CUR (3600−12000 mg/day) in patients with colorectal cancer could achieve efficient chemopreventive effect (*4*−*6*), the large dose of CUR and frequent administrations involved showed an increase of side effects and lower compliance from the users (*7*).

Delivery systems have been used to enhance the effectiveness of drug and food materials and to decrease the dosage required. Nanonization is one of the drug/food delivery processes that can help overcome a material's poor aqueous solubility, dissolution, and/or bioavailability (*8*, *9*). Nanoparticles are stable colloidal particles that range in size from 10 to 1000 nm. Many studies have demonstrated that reduction in particle size of the active ingredient to nanoparticle size can improve its efficacy, solubility, and bioavailability, such as seen in sirolimus, aprepitant, and fenofibrate (*10*).

The aim in the present study was to develop a novel curcumin nanoparticle system (CURN) using a simple nanoprecipitation technique with polyvinylpyrrolidone (PVP) as the hydrophilic carrier. The physicochemical characterization of CURN was evaluated by photon correlation spectroscopy (PCS), yield and encapsulation efficiency, transmission electron microscopy (TEM), powder X-ray diffraction (XRD), Fourier transform infrared spectroscopy (FT-IR), and dissolution study. In addition, the antioxidant and antihepatoma activities of CURN were assessed in comparison to those of free CUR by examining the free radical scavenging ability, antilipid peroxidation effect, and cytotoxicity against human hepatoma cell lines HepG2, PLC/PRF/5, and Hep3B.

MATERIALS AND METHODS

Chemical and Reagents. CUR, PVP, thiobarbituric acid, Tris-HCl, ferrous chloride, ascorbate, 2,2-diphenyl-1-picrylhydrazyl (DPPH), dimethyl sulfoxide (DMSO), and {sodium 3′-[1-(phenylaminocarbonyl)-3,4-tetrazolium]bis(4-methoxy-6-nitro)benzenesulfonic acid hydrate} (XTT) were obtained from Sigma (St. Louis, MO). Dulbecco's modified Eagle's medium (DMEM), penicillin G, streptomycin, and amphotericin B were purchased from GIBCO BRL (Gaithersburg, MD). All other chemical reagents were of analytical grade.

*Address correspondence to this author at the School of Pharmacy, College of Pharmacy, Kaohsiung Medical University, 100 Shih-Chuan first Road, Kaohsiung 807, Taiwan, ROC (telephone +886-7-3121101, ext. 2122; fax +886-7-3135215; e-mail aalin@kmu.edu.tw).

 Published on Web 05/20/2010

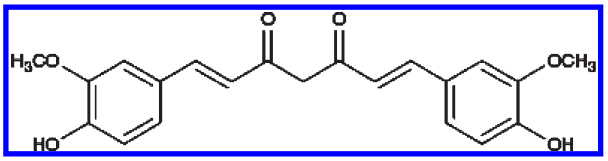

Figure 1. Chemical structure of curcumin.

Preparation of Curcumin Nanoparticles and Solutions. Curcumin nanoparticles (CURN) were prepared using the nanoprecipitation method (*11*, *12*). CUR (50 mg) was dissolved in 25 mL of ethanol. The organic phase solutions were quickly injected into 75 mL of an aqueous solution that contained 300 mg of PVP. During the injection process, the mixed solution was homogenized at 22000 rpm for 25 min. Following that, excess ethanol from the mixed solution was completely removed by rotary vacuum evaporation at 40 °C in a water bath. The remaining fraction (approximately 70 mL), which consists of the nanoparticle solution, was then used for particle size analysis or lyophilized and stored in a moisture-proof instrument for subsequent characterizations. In addition, a mixture made in a mortar with ratio of curcumin/PVP of 1:6 was also prepared as the curcumin physical mixture for physicochemical studies.

To prepare the control solution of curcumin in water (CURH), 100 mg of CUR was added to 10 mL of distilled water and then placed in a supersonic water bath for 10 min. Subsequently, the suspension was centrifuged at 1000 rpm for 10 min, and the supernatant was used as stock solution of CURH. For the preparation of curcumin in DMSO (CURD), 1 mg of CUR was dissolved with 1 mL of 100% DMSO and directly used as the stock solution of CURD.

CURH, CURD, and CURN were all diluted in a series of concentrations with water or medium for all experimental analyses. In all assays, the final concentration of DMSO in the CURD control group did not have any effect on the experimental results.

Morphology and Particle Size Analysis. The morphology of CURN was observed by transmission electron microscopy analysis (TEM) (JEM-2000EXII instrument, JEOL Co., Tokyo, Japan). The sample was stained with 0.5% (w/v) phosphotungstic acid and fixed on copper grids before analysis.

PCS was used for particle size analysis with an N5 Submicrometer Particle Size Analyzer (Beckman Coulter, Inc.). A 25 mW helium−neon laser lamp with a wavelength of 632.8 nm was employed to determine the particle size. The polydispersity index (PI) is a measure of the distribution broadness of the particle size, which was obtained by PCS analysis. Samples were diluted 10 times with distilled water before assessment.

HPLC Analysis of Curcumin. The high-performance liquid chromatography system consisted of a pump P-680, an autosampler ASI-100, and a UVD-170U detector. The LichroCART Purospher STAR (250 × 4.6 mm i.d., 5 μm) was used as an analytical column, and the temperature was kept at 37 °C. The mobile phase consisted of acetic acid, 10 mM phosphate buffer, and acetonitrile (1:50:50), and phosphoric acid was also included to adjust the pH value to 2.5. The flow rate was set at 0.8 mL/min. The wavelength of the UV detector was operated at 250 nm.

Yield and Encapsulation Efficiency of CURN. The yield and encapsulation efficiency were assessed to determine the loading dosage of curcumin in the CURN, and the experiments were performed according to a previously described method (*12*). Briefly, the appropriate amount of CURN was diluted with methanol. Then, the curcumin concentration and yield were measured by the above-mentioned HPLC method. For encapsulation efficiency, 500 μL of CURN was added into centrifugal filter devices (Microcon YM-10, Millipore) and then centrifuged at 10000 rpm for 30 min. Following that, the encapsulated (the supernatant liquor) and unencapsulated (the residual liquor) portions of CUR from CURN were separated.

Equations 1 and 2 were used to calculate the yield and encapsulation efficiency of CUR from CURN, respectively, as

$$\text{yield}\ (\%) = C_{\text{Cur}}(V_{\text{Cur}}/W_{\text{Cur}}) \times 100 \quad (1)$$

$$\text{encapsulation efficiency}\ (\%) = [(C_{\text{Cur}}V_{\text{Cur}}) - (F_{\text{Cur}}V_{\text{Cur}})]/C_{\text{Cur}}V_{\text{Cur}} \times 100 \quad (2)$$

where C_{Cur} is the concentration of CUR from CURN, W_{Cur} is the theoretical amount of CUR added, V_{Cur} is the volume of CUR from the CURN, and F_{Cur} is the concentration of CUR in the unencapsulated portion.

FT-IR Spectroscopy. FT-IR spectra were determined by a Perkin-Elmer 2000 spectrophotometer (Perkin-Elmer, Norwalk, CT). Potassium bromide (KBr) was mixed with each sample and ground by an agate mortar to be finally compressed into a thin tablet. The study was done in triplicate, and the scanning range was set between 400 and 4000 cm^{-1}.

Powder XRD. XRD patterns were recorded using a Siemens D5000 (Germany) with Cu Kα radiation at 40 kV and 80 mA. The scanned angle (2θ) was set from 2° to 50°, with the scanning rate at 1°/min. The study was done in triplicate.

Dissolution Study and HPLC Analysis of Curcumin and Its Nanoparticles. In vitro dissolution studies of CUR and its nanoparticle system were carried out in a pH 1.2 buffer solution (containing 50 mL of 0.2 M KCl, 85 mL of 0.2 M HCl, and 65 mL of distilled water) at 37 ± 0.5 °C (USP XXIV). Fifteen milligrams each of CUR and CURN was dissolved in 100 mL of dissolution medium, which was stirred by a paddle with a rotating rate of 100 rpm. Then, 0.5 mL of each sample was withdrawn at time intervals of 0, 5, 10, 20, 40, and 60 min. The concentration of CUR from each time point was determined by HPLC analysis.

DPPH Scavenging Activity. DPPH is a stable free radical that has been used to determine a compound's free radical scavenging activity (*13*, *14*). The DPPH scavenging effect was evaluated according to modified methods from Zou et al. (*14*). Briefly, CURN, CURH, and CURD were prepared at multiple concentrations. Then, 125 μL of a 200 μM DPPH ethanol solution was mixed with equivalent aliquots of different samples and subsequently incubated at room temperature in the dark. After 30 min, the absorbance of the reaction solution was measured by a microplate spectrophotometer (μQuant, Biotek Instruments, Winooski, VT) at 517 nm. The percent free radical scavenging activity from the sample was calculated using the following equation: % scavenging effect = $[(\text{control}_{517\text{nm}} - \text{sample}_{517\text{nm}})/\text{control}_{517\text{nm}}] \times 100$. The concentration of each sample reaching 50% of scavenging activity (SC_{50}) was used to compare the levels of free radical scavenging activity between samples.

Antilipid Peroxidation Assay. Lipid peroxidation in the liver homogenate was measured by the thiobarbituric acid reactive method according to Yen et al. (*15*). Liver tissue from Wistar rat was homogenized with ice-cold 150 mM Tris-HCl buffer (pH 7.4) using a Potter−Elvehjem homogenizer and prepared to 20% homogenate (w/v). CURN, CURH, and CURD were prepared at multiple concentrations. An amount of 50 μL of liver homogenate was mixed with 30 μL of test sample and then mixed with 10 μL of 4 mM $FeCl_2$ and 10 μL of 0.2 mM ascorbic acid in a 2 mL microtube for incubation at 37 °C for 60 min. Subsequently, 100 μL of 0.1 N HCl, 40 μL of 9.8% SDS, 180 μL of deionized water, and 400 μL of 0.6% TBA were successively added to each tube and vigorously shaken. These tubes were then placed at 95 °C for 30 min. After cooling, 1000 μL of *n*-butanol was added to each tube and centrifuged at 1000*g* for 25 min. The supernatant was subsequently measured with a microplate spectrophotometer (μQuant, Biotek Instruments) at 532 nm. The percentage of lipid peroxidation inhibition was calculated using the following equation: $[1 - (\text{induced}_{532\text{nm}} - \text{sample}_{532\text{nm}})/(\text{induced}_{532\text{nm}} - \text{control}_{532\text{nm}})] \times 100\%$. The inhibitory concentration that suppressed 50% of the lipid peroxide production was expressed as IC_{50}.

Cell Culture and Antihepatoma Activity Assay. The antihepatoma activity was evaluated by modified methods from Chiang et al. (*16*). The human hepatoma cell lines (American Type Culture Collection, Manassas, VA) HepG2 (HB-8065), PLC/PRF/5 (CRL-8024), and Hep3B (HB-8064) were cultured in DMEM supplemented with 10% fetal bovine serum and antibiotics (100 units/mL penicillin G, 100 μg/mL streptomycin, and 0.25 μg/mL amphotericin B) in an incubator at 37 °C with 5% CO_2. The viability of HepG2, PLC/PRF/5, and Hep3B cells was evaluated by the XTT assay. Briefly, cells were seeded in a 96-well culture plate with a density of 1×10^4 cells/well and then treated with CURH, CURD, or CURN at 20 μg/mL in DMEM medium for 48 h. At the end of the incubation, each well was washed twice with phosphate-buffered saline, and then 150 μL of XTT test solution (100 μL of DMEM, 50 μL of XTT-labeling reagent, and 1 μL of electron coupling reagent) was added to each well and further incubated for 4 h at 37 °C. The cell viability of the samples was finally measured with a microplate spectrophotometer (μQuant, Biotek Instruments) at a test wavelength of 492 nm and a reference wavelength of 690 nm.

Table 1. Mean Particle Size and Polydispersity Index of Curcumin (CUR) and Its Nanoparticles (CURN)[a]

	mean particle size (nm)	polydispersity Index
CUR	2363.10 ± 353.09	1.51 ± 0.32
CURN	142.90 ± 3.12 a	0.19 ± 0.07 a

[a] All determinations were performed in triplicate and values are expressed as mean ± SD, $n = 3$. "a" indicates significant difference from CUR ($P < 0.05$).

Statistical Analysis. All data are expressed as mean ± standard deviation. Statistical analysis was done with one-way analysis of variance (ANOVA) and Tukey's post hoc test using SPSS 13.0 software. $P < 0.05$ was considered to be statistically significant.

RESULTS AND DISCUSSION

Characterization of Curcumin Nanoparticles. CURN was prepared by a simple nanoprecipitation technique with PVP as the carrier. PVP is a strong hydrophilic polymer that has been applied to improve solubility and bioavailability of poor water-soluble compounds, because it delays the crystallization of compounds by forming molecular adducts (*17*, *18*). As **Table 1** shows, the mean particle diameters of CUR and CURN were 2362.10 ± 353.09 and 142.90 ± 3.12 nm and the polydispersity index (PI) values 1.51 ± 0.32 and 0.19 ± 0.07, respectively. When the PI value is <0.3, the indication is that the sample is of narrow distribution. On the contrary, the higher the PI value (>0.3) the broader the distribution of the particle sizes (*19*). These findings indicated that the small mean particle size and uniform particle distribution observed in CURN are associated with the presence of PVP. A possible explanation for this result is that the presence of PVP could reduce the particle size and size distribution of CUR. This phenomenon is consistent with the reports of Karavas et al. (*17*). In addition, the appearance of CURN was also observed as small spherical shapes with a uniform size distribution (**Figure 2**). Moreover, the yield (91.59 ± 4.49%) and encapsulation efficiency (99.93 ± 0.01%) of CURN also suggested that PVP was an optimal polymer for curcumin in the nanoparticle formulation.

Powder XRD and DSC analyses were applied to investigate the crystal transformation of the nanoparticle system. **Figure 3A** indicates the XRD patterns of CUR, PVP, physical mixture, and lyophilized CURN. The characteristic peaks of CUR appeared at a diffraction angle of 2θ (8.89°, 14.48°, 17.22°, 18.18°, 23.33°, 24.60°, and 25.52°), suggesting that the drug possessed a highly crystalline structure. In contrast, no characteristic peaks appeared in the patterns of the lyophilized CURN, suggesting a conversion of CUR from a highly crystalline condition to an amorphous state. PVP probably suppressed the crystal aggregates of CUR during the preparation of its nanoparticle system, thus promoting the formation of an amorphous complex. A similar finding has been demonstrated for piroxicam dispersed into PVP, which also displayed an amorphous state (*18*). On the other hand, as shown in **Figure 3B**, the melting point of CUR displayed an endothermic peak at 175 °C, and PVP showed a broad endothermic peak at around 80 °C. However, the physical mixture of CUR displayed a weak endothermic peak, which indicated that the crystalline structure of CUR is still present in the physical mixture. Moreover, the endothermic peak of CUR completely disappeared in the lyophilized CURN. This latter observation indicated that CUR was dispersed by nanoprecipitation into PVP to form a high-energy amorphous state.

The intermolecular interaction between CUR and the carrier was determined by FT-IR spectroscopy. **Figure 3C** shows the FT-IR spectra of CUR, PVP, and CURN. CUR displayed the characteristic intensities of the O−H stretch at 3508 cm^{-1}.

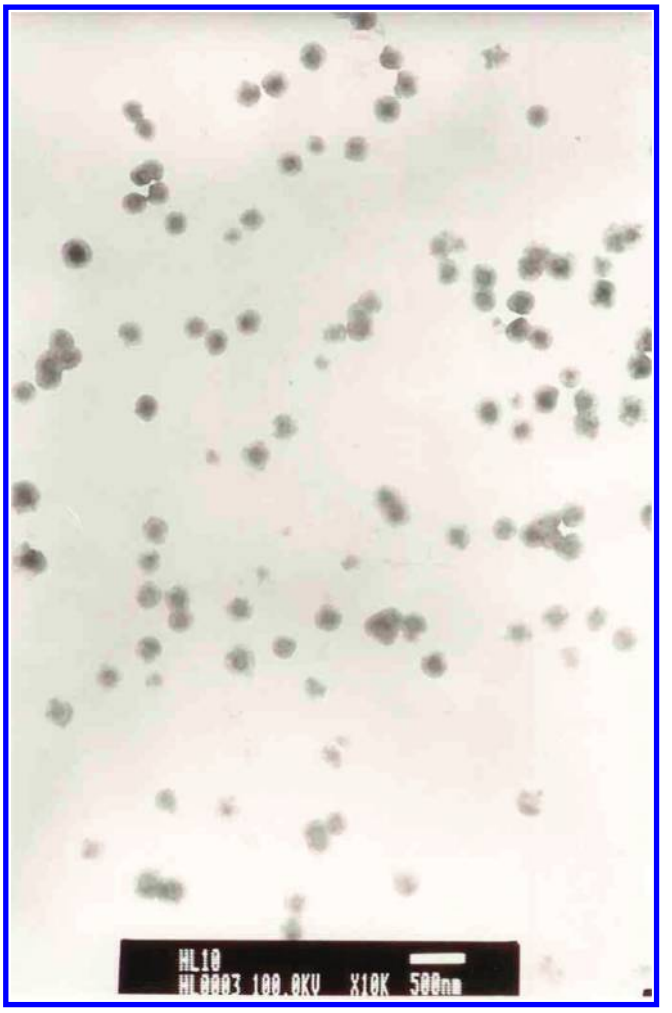

Figure 2. Morphology of the curcumin nanoparticles as shown by TEM photograph.

The spectrum of PVP displayed the C═O absorption band at 1662 cm^{-1}. In the case of CURN, the C═O absorption band of PVP was shifted to a lower wavenumber and the O—H absorption band of CUR was completely absent. This could be due to the formation of intermolecular hydrogen bonds between the O—H band of CUR and the C═O band of PVP. Tantishaiyakul et al. have previously pointed out that hydrogen bonding can influence the conversion of drug crystals (*20*).

Enhancement of Drug Release. Figure 4 indicates the dissolution profiles of CUR and its nanoparticles in simulated gastric medium (pH 1.2 buffer) at 60 min. The dissolution percentage at 60 min (D_{60min}) of pure CUR was <1%. Its hydrophobic characteristic probably resulted in the drug powder drifting on the surface of the pH 1.2 buffer solution, which prevented the wetting process from occurring between the drug surface and the medium. In contrast, the D_{60min} of CUR from its nanoparticles system was >99% under the same condition. The possible reason was that the absorption of PVP onto the surface of the drug crystals increased the surface wetting of the hydrophobic drug (*21*). In addition, the improvement in the dissolution percentage of CUR from its nanoparticle system could also be attributed to the reduction in particle size, the amorphous state transformation of its crystals that was confirmed by XRD and DSC results, and the formation of intermolecular interactions as depicted by the FT-IR results.

CURN Effectively Enhanced the Antioxidant Activities. Oxygen can be catalyzed by many oxidases, such as xanthine oxidase and

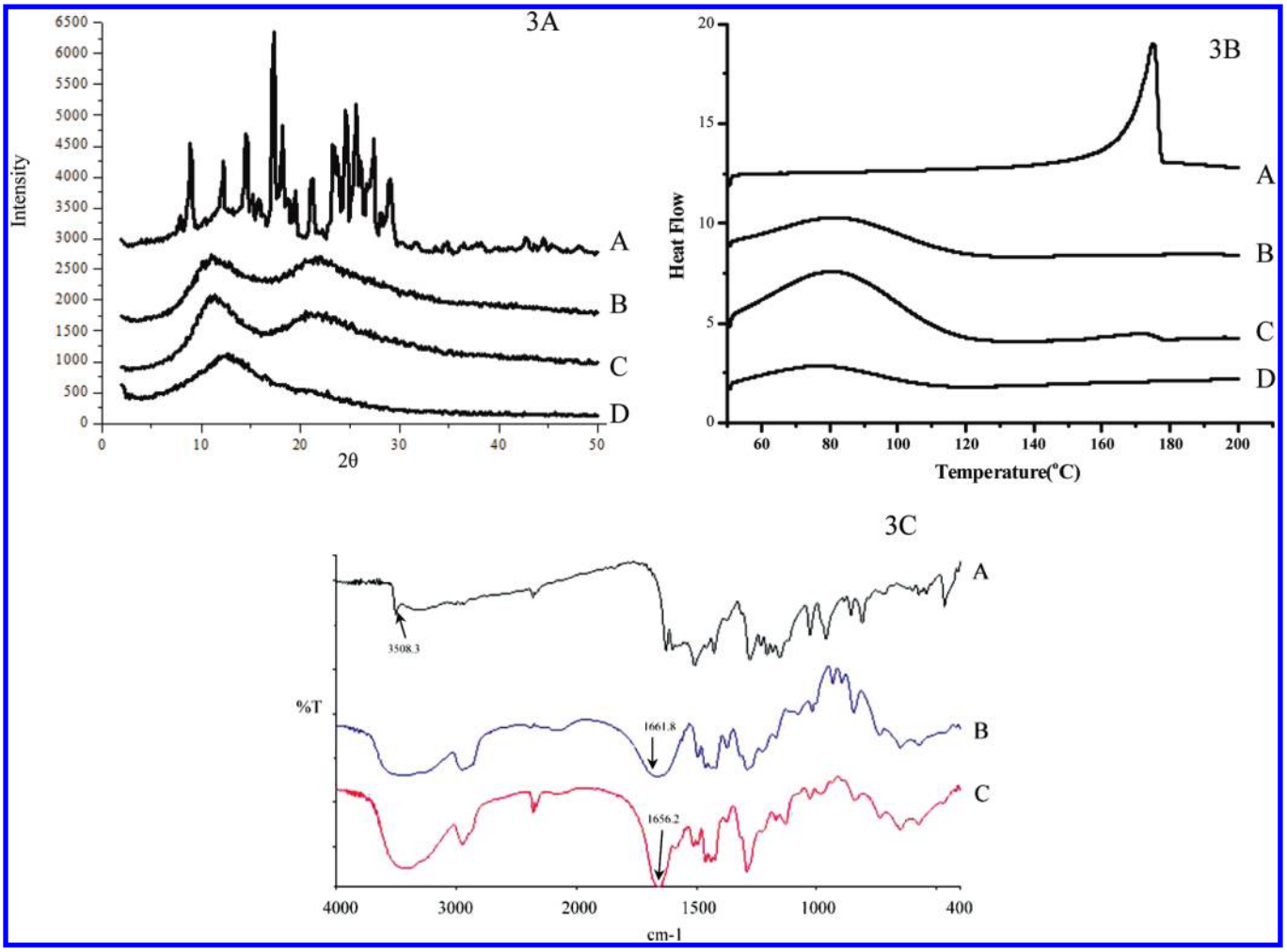

Figure 3. X-ray diffraction (**A**) and DSC (**B**) patterns of curcumin, its physical mixture, and its nanoparticles: (A) curcumin (CUR); (B) curcumin nanoparticles (CURN); (C) curcumin physical mixture; (D) PVP. FT-IR spectra (**C**) of curcumin, its physical mixture, and its nanoparticles: (A) CUR; (B) CURN; (C) PVP. Results are representative from three independent experiments.

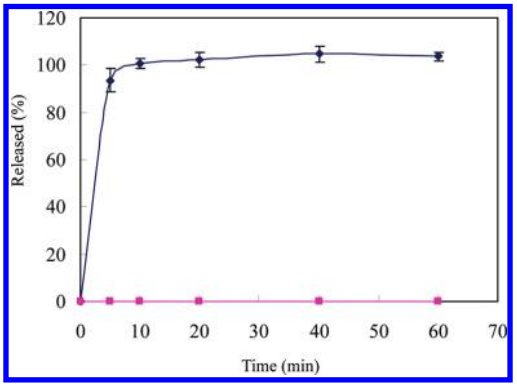

Figure 4. Dissolution profiles of curcumin and its nanoparticles: CUR (●); CURN (◆). Values are expressed as mean ± SD, n = 5, from three independent experiments.

NADPH oxidase, and also be converted to a common free radical, superoxide anion ($O_2^{\bullet-}$). $O_2^{\bullet-}$ is metabolized by antioxidant enzymes including superoxide dismutase, catalase, and glutathione peroxidase and then converted to hydrogen peroxide (H_2O_2) and water, respectively, under normal conditions in the human body. Unfortunately, oxidative stress can be produced due to an excess of superoxide anions that participate in the Fenton reaction, which generates the most toxic free radical, the hydroxyl radical ($^{\bullet}OH$). These free radicals are pro-oxidant and are generally referred to as reactive oxygen species (ROS). It has been well established that ROS can react with the lipid layer of the cell membrane, thereby resulting in lipid peroxidation, and they can also attack DNA and protein, which could induce cell death leading to various diseases.

Many natural foods contain active compounds that are antioxidants and have been used to prevent and/or help cure diseases. CUR is one such dietary antioxidant and food supplement. Previous studies have demonstrated that the antioxidant activity of CUR is attributed to its structure−activity relationship (SAR). The CUR basic structure consists of two methoxylated phenols and an enol from a β-diketone moiety (*22*). The phenolic OH group and the hydrogen abstraction from the methylene CH_2 group are responsible for the increase in antioxidant activity of CUR (*23*, *24*).

In the present study, the antioxidant activities were determined by DPPH free radical scavenging and antilipid peroxidation assays. The results on the DPPH scavenging ability from CURH, CURD, and CURN are shown in **Figure 5A**. No statistical significance between CURN (18.08 ± 0.54 μg/mL) and CURD (21.43 ± 0.63 μg/mL) was observed, suggesting that CURN had the same DPPH free radical scavenging efficiency as DMSO-dissolved CUR. However, when CURN was compared with CURH, the nanonized compound was 1034-fold stronger than the water preparation of pure CUR (18689.41 ± 162.20 μg/mL) ($P < 0.05$). This observation indicated that CUR from the water-soluble

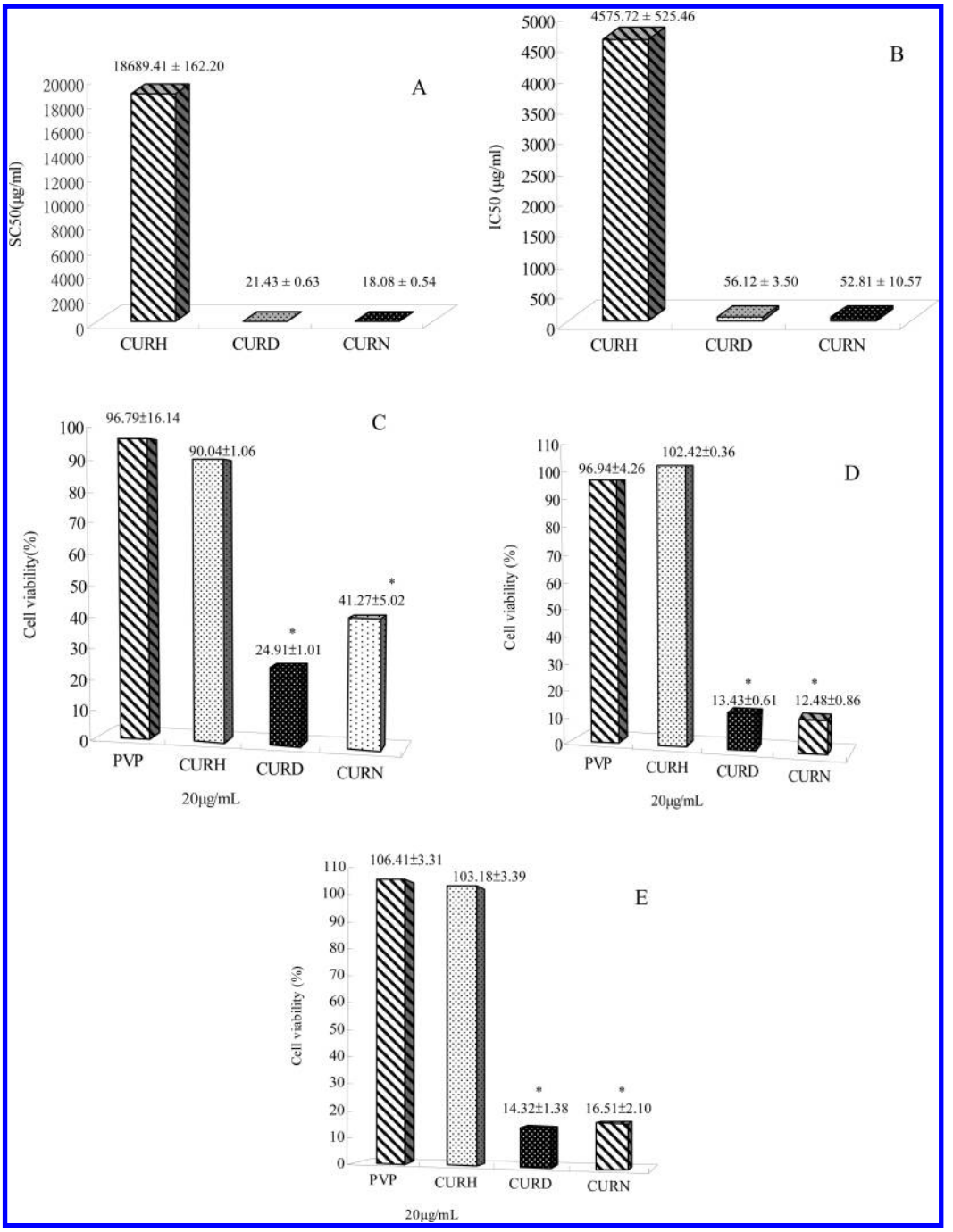

Figure 5. Antioxidant and antihepatoma activities of CURH, CURD, and CURN: (A) DPPH radical scavenging activity; (**B**) antilipid peroxidation; and cytotoxicity on human HepG2 (**C**), PLC/PRF/5 (**D**), and Hep3B (**E**) cells. CURH, curcumin dissolved in water; CURD, curcumin dissolved in DMSO.; CURN, curcumin nanoparticles dissolved in water. All determinations were performed in triplicate, and values are expressed as mean ± SD, $n = 3$. #, significantly different from CURH ($P < 0.05$, Tukey's post hoc test).

nanoparticle system at low concentration could achieve efficient DPPH free radical scavenging activity.

The inhibitory effect on $FeCl_2$/ascorbate-induced lipid peroxidation in rat liver homogenate was used to evaluate the antilipid peroxidation activity of the different CUR systems (CURH, CURD, and CURN), and the results are shown in **Figure 5B**. Again, CURN (52.81 ± 10.57 μg/mL) had similar efficiency in antilipid peroxidation activity when compared with CURD (56.12 ± 3.50 μg/mL), but was 87-fold more efficient than CURH (4575.72 ± 525.46 μg/mL) ($P < 0.05$). Schaffazick et al. have previously reported a similar effect in which the nanoparticle system increased the antioxidant ability of melatonin antilipid peroxidation (*25*).

CURN Effectively Enhanced the Antihepatoma Activity. It is well established that CUR can induce apoptosis or cell cycle arrest in human cancer cell lines, including gastric, lung, pancreatic, hepatocellular, epithelial, and breast carcinoma cells, and also lymphocytic leukemia cells. CUR can induce DNA damage to both the mitochondrial DNA and the nuclear DNA in hepatoma cells (*26*). Recently, a clinical study indicated that a single high-dose of CUR (8000 mg/day) in humans produced a biological effect for the chemoprevention of cancer (*27*). Despite the low bioavailability of the orally administered high dose of CUR, the anticancer effect was promising.

To estimate the inhibitory effects of different CUR systems on hepatoma cell proliferation, we determined the viability of

HepG2, PLC/PRF/5, and Hep3B cells that were treated with different CUR preparations (CURH, CURD, and CURN) for 48 h. Results from the cytotoxicity assay showed that CURN effectively suppressed HepG2 (41.27 ± 5.02%, **Figure 5C**), PLC/PRF/5 (12.48 ± 0.86%, **Figure 5D**), and Hep3B (16.51 ± 2.10%, **Figure 5E**) cell growth with similar efficiency as CURD. On the contrary, CURH did not display any cytotoxicity in any of the cell lines (HepG2, 90.04 ± 1.06%, **Figure 5C**; PLC/PRF/5, 102.42 ± 0.36%, **Figure 5D**; or Hep3B, 103.18 ± 3.39%, **Figure 5E**), whereas CURN effectively achieved an antihepatoma effect when compared with CURH at 20 μg/mL ($P < 0.05$). The increased efficiency in suppressing hepatoma cell growth by nanonized compounds has also been observed in the study by Liang et al. (*28*), in which the paclitaxel nanoparticle system could effectively inhibit the growth of HepG2 cells.

In conclusion, a novel curcumin nanoparticle system (CURN) was successfully developed by a simple nanoprecipitation technique with the hydrophilic carrier PVP. Our study also demonstrated that the physicochemical properties of curcumin from the nanoparticle system have been improved including a reduction in compound particle size, the formation of a high-energy amorphous state, and the induction of intermolecular hydrogen bonding, which altogether enhanced its water solubility and drug release. Furthermore, the more efficient antioxidant and anticancer effects of CURN compared to the CUR water preparation are likely due to the increase of drug release property. Whereas DMSO is widely used to improve compound solubility in many laboratory studies, its clinical application to improve drug solubility is rather limited due to several systemic side effects, including vomiting, diarrhea, hemolysis, hypertension, bradycardia, and heart block (*29*, *30*). In contrast, our attempt in nanonizing the insoluble curcumin to improve its dissolution profile represents an attractive alternative to DSMO in solubilizing this compound. Our results clearly show that the nanonized curcumin, which dissolves readily in water, can achieve a very similar efficiency profile in terms of antioxidant and anticancer activities in comparison to DMSO-dissolved curcumin. Consequently, we suggest that CURN could help improve the bioavailability of curcumin and lower its dosage. Thus, the use of curcumin nanoparticles merits further studies for clinical application.

LITERATURE CITED

(1) Goel, A.; Kunnumakkara, A. B.; Aggarwal, B. B. Curcumin as "curecumin": from kitchen to clinic. *Biochem. Pharmacol.* **2008**, *75*, 787–809.

(2) Pari, L.; Tewas, D.; Eckel, J. Role of curcumin in health and disease. *Arch. Physiol. Biochem.* **2008**, *114*, 127–149.

(3) Anand, P.; Kunnumakkara, A. B.; Newman, R. A.; Aggarwal, B. B. Bioavailability of curcumin: problems and promises. *Mol. Pharmaceutics* **2007**, *4*, 807–818.

(4) Garcea, G.; Jones, D. J.; Singh, R.; Dennison, A. R.; Farmer, P. B.; Sharma, R. A.; Steward, W. P.; Gescher, A. J.; Berry, D. P. Detection of curcumin and its metabolites in hepatic tissue and portal blood of patients following oral administration. *Br. J. Cancer* **2004**, *90*, 1011–1015.

(5) Sharma, R. A.; McLelland, H. R.; Hill, K. A.; Ireson, C. R.; Euden, S. A.; Manson, M. M.; Pirmohamed, M.; Marnett, L. J.; Gescher, A. J.; Steward, W. P. Pharmacodynamic and pharmacokinetic study of oral *Curcuma* extract in patients with colorectal cancer. *Clin. Cancer Res.* **2001**, *7*, 1894–1900.

(6) Steward, W. P.; Gescher, A. J. Curcumin in cancer management: Recent results of analogue design and clinical studies and desirable future research. *Mol. Nutr. Food Res.* **2008**, *52*, 1005–1009.

(7) Lao, C. D.; Ruffin, M. T.; Normolle, D.; Heath, D. D.; Murray, S. I.; Bailey, J. M.; Boggs, M. E.; Crowell, J.; Rock, C. L.; Brenner, D. E. Dose escalation of a curcuminoid formulation. *BMC Complement. Altern. Med.* **2006**, *6*, 10–14.

(8) Devalapally, H.; Chakilam, A.; Amiji, M. M. Role of nanotechnology in pharmaceutical product development. *J. Pharm. Sci.* **2007**, *96*, 2547–2565.

(9) Ratnam, D. V.; Ankola, D. D.; Bhardwaj, V.; Sahana, D. K.; Kumar, M. N. Role of antioxidants in prophylaxis and therapy: a pharmaceutical perspective. *J. Controlled Release* **2006**, *113*, 189–207.

(10) Kesisoglou, F.; Panmai, S.; Wu, Y. Nanosizing-oral formulation development and biopharmaceutical evaluation. *Adv. Drug Delivery Rev.* **2007**, *59*, 631–644.

(11) Bilati, U.; Allémann, E.; Doelker, E. Development of a nanoprecipitation method intended for the entrapment of hydrophilic drugs into nanoparticles. *Eur. J. Pharm. Sci.* **2005**, *24*, 67–75.

(12) Wu, T. H.; Yen, F. L.; Lin, L. T.; Tsai, T. R.; Lin, C. C.; Cham, T. M. Preparation, physicochemical characterization, and antioxidant effects of quercetin nanoparticles. *Int. J. Pharm.* **2008**, *346*, 160–168.

(13) Sun, T.; Xu, Z.; Wu, C. T.; Janes, M.; Prinyawiwatkul, W.; No, H. K. Antioxidant activities of different colored sweet bell peppers (*Capsicum annuum* L.). *J. Food Sci.* **2007**, *72*, S98–102.

(14) Zou, Y.; Lu, Y.; Wei, D. Antioxidant activity of a flavonoid-rich extract of *Hypericum perforatum* L. in vitro. *J. Agric. Food Chem.* **2004**, *52*, 5032–5039.

(15) Yen, F. L.; Wu, T. H.; Lin, L. T.; Cham, T. M.; Lin, C. C. Concordance between antioxidant activities and flavonol contents in different extracts and fractions of *Cuscuta chinensis*. *Food Chem.* **2008**, *108*, 455–462.

(16) Chiang, L. C.; Ng, L. T.; Lin, I. C.; Kuo, P. L.; Lin, C. C. Antiproliferative effect of apigenin and its apoptotic induction in human Hep G2 cells. *Cancer Lett.* **2006**, *237*, 207–214.

(17) Karavas, E.; Georgarakis, M.; Docoslis, A.; Bikiaris, D. Combining SEM, TEM, and micro-Raman techniques to differentiate between the amorphous molecular level dispersions and nanodispersions of a poorly water-soluble drug within a polymer matrix. *Int. J. Pharm.* **2007**, *340*, 76–83.

(18) Wu, K.; Li, J.; Wang, W.; Winstead, D. A. Formation and characterization of solid dispersions of piroxicam and polyvinylpyrrolidone using spray drying and precipitation with compressed antisolvent. *J. Pharm. Sci.* **2009**, *98*, 2422–2431.

(19) Yen, F. L.; Wu, T. H.; Lin, L. T.; Cham, T. M.; Lin, C. C. Nanoparticles formulation of *Cuscuta chinensis* prevents acetaminophen-induced hepatotoxicity in rats. *Food Chem. Toxicol.* **2008**, *46*, 1771–1777.

(20) Tantishaiyakul, V.; Kaewnopparat, N.; Ingkatawornwong, S. Properties of solid dispersions of piroxicam in polyvinylpyrrolidone. *Int. J. Pharm.* **1999**, *181*, 143–151.

(21) Gupta, V. R.; Mutalik, S.; Patel, M. M.; Jani, G. K. Spherical crystals of celecoxib to improve solubility, dissolution rate and micromeritic properties. *Acta. Pharm.* **2007**, *57*, 173–184.

(22) Masuda, T.; Toi, Y.; Bando, H.; Maekawa, T.; Takeda, Y.; Yamaguchi, H. Structural identification of new curcumin dimers and their contribution to the antioxidant mechanism of curcumin. *J. Agric. Food Chem.* **2002**, *50*, 2524–2530.

(23) Priyadarsini, K. I.; Maity, D. K.; Naik, G. H.; Kumar, M. S.; Unnikrishnan, M. K.; Satav, J. G.; Mohan, H. Role of phenolic O−H and methylene hydrogen on the free radical reactions and antioxidant activity of curcumin. *Free Radical Biol. Med.* **2003**, *35*, 475–484.

(24) Venkatesan, P.; Rao, M. N. Structure−activity relationships for the inhibition of lipid peroxidation and the scavenging of free radicals by synthetic symmetrical curcumin analogues. *J. Pharm. Pharmacol.* **2000**, *52*, 1123–1128.

(25) Schaffazick, S. R.; Pohlmann, A. R.; de Cordova, C. A.; Creczynski-Pasa, T. B.; Guterres, S. S. Protective properties of melatonin-loaded nanoparticles against lipid peroxidation. *Int. J. Pharm.* **2005**, *289*, 209–213.

(26) Cao, J.; Jia, L.; Zhou, H. M.; Liu, Y.; Zhong, L. F. Mitochondrial and nuclear DNA damage induced by curcumin in human hepatoma G2 cells. *Toxicol. Sci.* **2006**, *91*, 476–483.

(27) Cheng, A. L.; Hsu, C. H.; Lin, J. K.; Hsu, M. M.; Ho, Y. F.; Shen, T. S.; Ko, J. Y.; Lin, J. T.; Lin, B. R.; Ming-Shiang, W.; Yu, H. S.;

Jee, S. H.; Chen, G. S.; Chen, T. M.; Chen, C. A.; Lai, M. K.; Pu, Y. S.; Pan, M. H.; Wang, Y. J.; Tsai, C. C.; Hsieh, C. Y. Phase I clinical trial of curcumin, a chemopreventive agent, in patients with high-risk or pre-malignant lesions. *Anticancer Res.* **2001**, *21*, 2895–2900.

(28) Liang, H. F.; Chen, S. C.; Chen, M. C.; Lee, P. W.; Chen, C. T.; Sung, H. W. Paclitaxel-loaded poly(γ-glutamic acid)-poly(lactide) nanoparticles as a targeted drug delivery system against cultured HepG2 cells. *Bioconjugate Chem.* **2006**, *17*, 291–299.

(29) Swanson, B. N. Medical use of dimethyl sulfoxide. *Rev. Clin. Basic Pharm.* **1985**, *5*, 1–33.

(30) Willhite, C. C.; Katz, P. I. Toxicology update: dimethyl sulfoxide. *J. Appl. Toxicol.* **1984**, *4*, 155–160.

Received for review January 13, 2010. Revised manuscript received March 19, 2010. Accepted April 29, 2010. This study was supported by the National Science Council of Taiwan (NSC 98-2313-B-037-001).